Molecular Cancer Therapeutics

AMPK and Akt Determine Apoptotic Cell Death following Perturbations of One-Carbon Metabolism by Regulating ER Stress in Acute Lymphoblastic Leukemia

Jeffim N. Kuznetsov[1], Guy J. Leclerc[2], Gilles M. Leclerc[2], and Julio C. Barredo[1,2,3]

Abstract

AICAr is a cell-permeable nucleotide that has been used *in vivo* and *in vitro* to activate AMPK. Our previous findings have shown that AICAr as a single agent induces dose- and time-dependent growth inhibition in acute lymphoblastic leukemia (ALL) cell lines. In addition, the combination of AICAr with antifolates [methotrexate (MTX) or pemetrexed] has been shown to further potentiate AMPK activation and to lead to greater cytotoxicity and growth inhibition in leukemia and other malignant cell types. Our data presented herein show that sustained endoplasmic reticulum (ER) stress is the predominant mechanism behind the synergistic induction of cell death by the combination of AICAr plus the inhibitor of one-carbon metabolism, MTX, in Bp- and T-ALL, as evidenced by induction of several unfolded protein response markers leading to apoptosis. We also show for the first time that AICAr in combination with MTX significantly induces Akt phosphorylation in ALL. Under these conditions, the concomitant inhibition of Akt, a cellular antagonist of AMPK, leads to further upregulation of AMPK activity and alleviates AICAr plus MTX-induced ER stress and apoptosis. Therefore, we also show that the concomitant activation of AMPK actually rescues the cells from AICAr plus MTX-induced ER stress and apoptosis. Our data suggest that the effects of AMPK activation on cell death or survival differ contextually depending on its signaling alterations with related oncogenic pathways and provide insight into the reported paradoxical proapoptotic versus prosurvival effects of AMPK activation. *Mol Cancer Ther; 10(3); 437–47. ©2011 AACR.*

Introduction

Acute lymphoblastic leukemia (ALL) is the most common hematological malignancy affecting children and adolescents and is the number one cause of cancer related mortality in this age group (1). Although cure rates for children with ALL have improved significantly, with an average of 80% survival, event-free survival (EFS) for children and adults diagnosed with chemotherapy resistant phenotypes of ALL or after relapse, continues to be dismal (EFS ∼10%–20%; refs. 2, 3). Current chemotherapy treatment intensification strategies and/or the use of stem cell transplantation have led to marginal improvements with limited impact on cure rates (3). These facts highlight the need to develop novel molecularly targeted therapies based on an understanding of pathways that are important for cell growth, proliferation, and survival.

AMP activated protein kinase (AMPK) is a highly conserved heterotrimeric serine/threonine protein kinase that regulates the intracellular ratio of AMP to ATP, and it is activated under conditions that deplete cellular ATP and increase AMP levels, such as glucose deprivation, heat shock, hypoxia, and ischemia (4, 5). It consists of a catalytic (α) and 2 regulatory (β and γ) subunits, and requires a conformational change induced by allosteric AMP binding to the α and γ subunits, which in turn allows its phosphorylation at Thr-172 of the α subunit by an upstream protein kinase (6). Consequently, compounds that act as AMP analogues can also induce the conformational change required for AMPK activation under conditions that do not involve changes in the ratio of AMP/ATP. One such compound is AICA riboside (AICAr), a cell-permeable nucleoside that is metabolically converted by adenosine kinase to AICA ribotide (AICAR, ZMP), a purine precursor that also exerts cellular effects as a 5′-AMP analogue.

AICAr has been used both *in vitro* (intact cells) and *in vivo* (whole animals) to induce AMPK activation [reviewed in (7)]. However, a major shortcoming of AICAr is that relatively high concentrations (>200 μmol/L) of the drug are necessary to exert cytotoxic effects (8). A potential strategy to overcome this difficulty or to induce synergy is to combine it with drugs that inhibit one-carbon metabolism such as methotrexate (MTX), which blocks

Authors' Affiliations: [1]Department of Biochemistry and Molecular Biology and [2]Department of Pediatrics, and [3]Sylvester Comprehensive Cancer Center, University of Miami Miller School of Medicine, Miami, Florida

Corresponding Author: Julio C. Barredo, Toppel Chair in Pediatric Hematology/Oncology, University of Miami Miller School of Medicine, 1580 NW 10 Ave, Miami, FL 33136. E-mail: jbarredo@med.miami.edu

doi: 10.1158/1535-7163.MCT-10-0777

the conversion of AICAR to formyl-AICAR and prevents its subsequent incorporation into the *de novo* purine biosynthesis pathway. MTX leads to an increased endogenous pool of AICAR and subsequently increases AMP accumulation through inhibition of AMP deaminase and adenosine deaminase (9). Thus, MTX is thought to exert a 2-pronged approach to activating AMPK by increasing both the endogenous pool of AICAR and the ratio of AMP/ATP. In addition, ATP, a purine-based nucleotide, inhibits AMPK activity through intrasteric interaction with both α and γ subunits and blocks AMPK activation by AMP (10).

As the master cellular energy switch, AMPK activation promotes catabolic processes while inhibiting energy-consuming anabolic metabolism. In this capacity, AMPK is known to phosphorylate/inhibit Acetyl-CoA carboxylase (ACC) at Ser79, which, in turn, relieves the inhibitory effects of ACC on fatty acid oxidation, an important ATP-producing process (4). AMPK is also known to inhibit phosphorylation of mTOR at its activating residue Ser 2448, thereby shutting down protein synthesis, an ATP-consuming process (5). Our laboratory was the first to show that AICAr induces dose- and time-dependent growth inhibition in Bp- and T-ALL cells, which occurs concomitantly with activation of AMPK, phosphorylation of ACC, downregulation of mTOR, and upregulation of p53 and p27 (8). Recent reports have shown that pretreatment of breast cancer, epidermoid carcinoma, and prostate cancer cell lines with MTX significantly potentiates AICAr-induced cell growth inhibition and cell death through increased AMPK activation (11). Pemetrexed, a multitargeted antifolate similar to MTX, in combination with AICAr also causes enhanced cell growth inhibition in CCRF-CEM (T-ALL) cells and correlates with AMPK activation and mTOR inhibition (12). In this study we further characterize the mechanisms of cell death induced by the combination of MTX plus AICAr, and the role of AMPK and Akt in determining cell death. We found that the effects of AMPK activation differ contextually depending on signaling alterations in related pathways, and provide insights into the reported paradoxical proapoptotic and prosurvival effects of AMPK activation.

Materials and Methods

Cell lines and chemicals

CCRF-CEM (T-lineage ALL) and NALM6 (B-lineage precursor Bp-ALL) were obtained in May 2009 from ATCC and DSMZ, respectively. Cells lines were authenticated by the manufacturer (ATCC and DSMZ), were frozen upon receipt and resuscitated every 4 months, using the original frozen stock. Cells were maintained in RPMI 1640 medium (Mediatech.) supplemented with 10% FBS (Invitrogen) and antibiotics at 37°C and 5% CO_2 atmosphere, and all drug treatments were done in the presence of FBS. AICAr was purchased from Toronto Research Chemicals, MTX from Sigma-Aldrich Corp., Akt inhibitor X (AIX) from EMD Chemicals Inc., Salubrinal from Enzo Life Sciences, and *N*-Acetyl-L-cysteine (NAC) from Sigma Aldrich. Accumulation of reactive oxygen species (ROS) was measured using STA-342 Oxi-Select ROS Assay Kit Cell Biolabs.

Cell proliferation assays

Nalm6 and CCRF-CEM cell lines were grown to mid log phase cultures, diluted to 0.5 × 106 cells/mL, and treated for 24, 48, and 72 hours with each drug alone or in combination. Apoptosis was evaluated using the Annexin V-FITC/PI Apoptosis Detection Kit I following the manufacturer's recommendations (BD Biosciences) and analyzed by flow cytometry. For temporary inhibition of Akt with AIX, cells were treated for 24 hours, washed with PBS 1X, and resuspended in drug-free media. We used this experimental design in this set of studies in order to assess if commitment to cell death occurred early after drug treatment, and apoptosis was measured following 24 hours of drug exposure, and following an additional 24 hours of incubation in drug-free media. For these experiments AICAr was used at 200 μmol/L; AIX at 12 μmol/L; MTX at EC50 concentrations, that is, 100 nmol/L and 50 nmol/L for CCRF-CEM and Nalm6 cells, respectively. Salubrinal at 10 μmol/L was used to inhibit endoplasmic reticulum (ER) stress, and NAC at 5 mmol/L for Nalm6 and 2 mmol/L for CCRF-CEM in rescue experiments following induction of ROS by AICAr and MTX for a total of 72 hours.

Immunoblots

AICAr, MTX, or AICAr plus MTX treated cells were harvested at the specified time points, washed with PBS 1X, and sonicated in 50 mmol/L Tris-HCl (pH 7.4) containing protease cocktail inhibitors (Thermo). Proteins (50 μg/lane) were resolved by SDS-PAGE electrophoresis and transferred onto PVDF membranes as previously described following manufacturer's recommendation (8). Proteins were detected using the enhanced chemiluminescence (ECL) detection kit (Amersham Biosciences).

Lentiviral transduction

Lentiviral particles carrying Scramble shRNA (sc-108080) and AMPKα1 shRNA (sc-29673-V) were obtained from Santa Cruz Biotechnology. Aliquots of 2×10^5 cells, grown in RPMI 1640 media to log phase cultures and resuspended in 1 mL media, were placed in 2 mL Falcon tubes and spun in the presence of 4 μg/mL polybrene and lentiviral particles (MOI = 5) for 20 minutes at 20°C and 2,000 RPM in desktop Beckman centrifuge GS-6R. The cells were resuspended in the polybrene+lentivirus media, incubated for 24 hours, then washed and resuspended in polybrene-free RPM1 media, and incubated for additional 48 hours at 37°C. Puromycin was added 72 hours after transduction at the initial concentration of 2 μg/mL, which was gradually increased to 6 μg/mL to select for stable transductants. Western Blot was

used to confirm total AMPK knockdown in ALL transductants (~75%–85%). ALL cell lines were grown to log phase cultures and were then diluted to 0.5 × 106 cells/mL and treated for 24 hours with each drug alone or in combination. After 24 hours of incubation, both drugs were washed, and cells were resuspended in drug-free media. Cell death was assessed by trypan blue exclusion using the ViCell XR cell viability analyzer (Beckman Coulter). This shorter incubation design (24 hours) was used for these experiments too, to evaluate if commitment to cell death occurred early during treatment.

Statistical analysis

Multiple comparisons of cell proliferation and cell viability/death were assessed by 1-way ANOVA followed by the Newman–Keuls multiple comparison test. Pair comparisons were achieved using a 2-tailed, paired *t* test of correlated samples using the Graph Pad PRISM software version 2 (GraphPad Software, Inc.). The data are expressed as mean ± SE.

Results

AICAr potentiates MTX-induced cytotoxicity in ALL cells lines

Our laboratory had previously shown that AICAr inhibited cell proliferation and induced cell cycle arrest and apoptosis in several ALL cell models (8). Others have shown that MTX can enhance the cytotoxic effects of AICAr in breast cancer, epidermoid carcinoma, and prostate cancer cell lines (11). Herein, we tested whether AICAr in combination with MTX exerted increased cytotoxicity in representative Bp- and T-ALL cell line models. AICAr was used at a concentration of 200 μmol/L for both cell lines, whereas MTX was used at EC50 concentrations for each cell line, that is 100 nmol/L for CCRF-CEM (T-ALL) and 50 nmol/L for Nalm6 (Bp-ALL) cells. Due to differences in intracellular metabolism of antifolates between Bp- and T-ALL, the former are known to be more sensitive to MTX (13). Our data show that MTX in combination with AICAr inhibited cell proliferation (data not shown) and induced significantly higher apoptotic cell death in both CCRF-CEM (Fig. 2A; $P < 0.01$) and Nalm6 (Fig. 2B; $P < 0.01$ and $P < 0.02$ for 24 and 48 hours, respectively) cell line models, compared with each drug alone. Although the combination MTX plus AICAr induced similar degree of apoptosis in both cell lines, this effect was apparent at 24 hours in Nalm6 cells whereas only at 48 hours in CCRF-CEM cells [likely due to lower FPGS expression and lengthier exposure required for sufficient accumulation of the active polyglutamated metabolites of MTX (MTX-PG) in CCRF-CEM cells; 14]. In addition, our data show that AICAr was also able to overcome the known relative resistance of CCRF-CEM cells to single agent MTX, which is shown by the ability of this combination to induce the same degree of cell death in both CCRF-CEM (MTX resistant) and Nalm6 (MTX sensitive) cells at 72 hours with the combination.

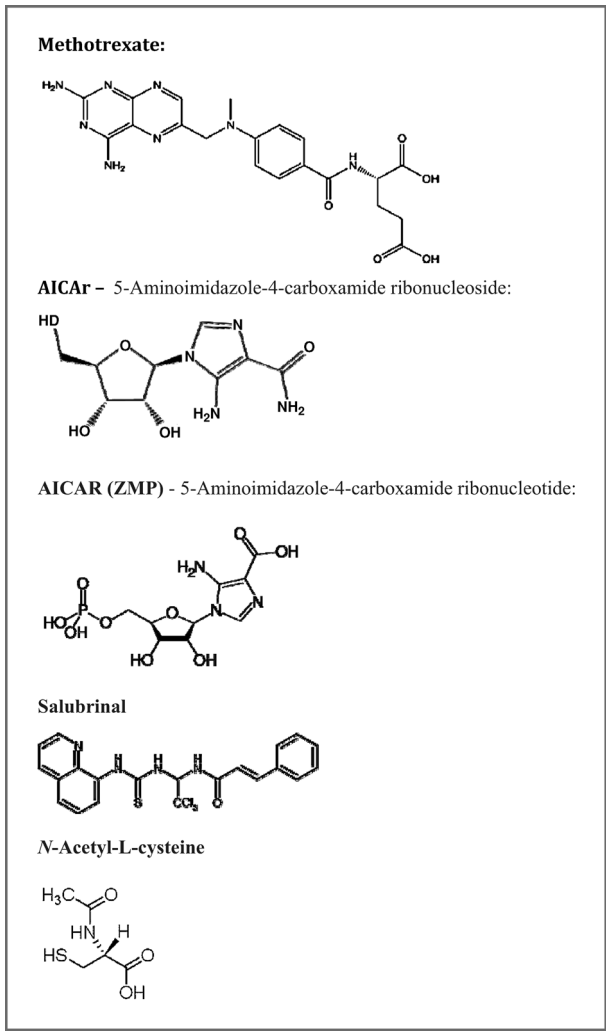

Figure 1. Chemical structures of compounds used in this study.

MTX potentiates AICAr-induced AMPK activation, downstream mTOR downregulation, and Akt activation

Our previous findings indicated that AMPK activation plays a key role in AICAr-induced ALL cytotoxicity. Therefore, we determined whether the increased induction of apoptosis and cell growth inhibition exhibited by cells treated with the combination of AICAr plus MTX resulted from enhanced AMPK activation. The effects of AICAr, MTX, and the combination AICAr plus MTX on the phosphorylation of AMPK, ACC, and mTOR, were examined by Western blot analysis in CCRF-CEM and Nalm6 cells following 6 hours and 24 hours drug exposure. These early time points were chosen to determine if signaling alterations and ensuing commitment to cell death occurred early during drug treatment. We found

that in both ALL cell lines, AMPK phosphorylation/activation at Thr172 was greater after treatment with the combination of AICAr plus MTX compared with single drug treatment, and led to a more robust inhibition of p-mTOR (decreased p-mTOR Ser2448; Fig. 2C). Expression of p-ACC (Ser79), a surrogate measure of AMPK activity, was also significantly increased following combination treatment. We repeatedly observed that AICAr plus MTX-induced AMPK activation seemed most pronounced in CCRF-CEM cells at the earlier time point (6 hours) and returned to baseline at 24 hours for the combination compared with Nalm6 cells. The biological relevance of this finding is not clear as the downstream effects of AMPK activation on p-ACC and p-mTOR persisted in both cell lines (Fig. 2C). Nevertheless, this signaling pattern would be consistent with the constitutive activation of Akt signaling, a known AMPK cellular antagonist, in the PTEN mutant CCRF-CEM cells (15).

Our published data show that AICAr induces phosphorylation of Akt at Ser473 in a dose-dependent manner, and this represents a compensatory survival mechanism in cells exposed to AICAr (8). Therefore, we investigated the effects of the combination of AICAr plus MTX on the expression of p-Akt. Western blot analysis of lysates from cells treated with AICAr, MTX, and the combination has shown that treatment with AICAr plus MTX significantly potentiates AICAr-induced Akt phosphorylation in both ALL cell lines (Fig. 2C). As expected, baseline levels of p-Akt were higher in the PTEN mutant CCRF-CEM cells when compared with the WT PTEN Nalm6 cells (Fig. 2C). We concluded that the increased expression of p-Akt resulted in part from increased level of AMPK activity on IGF1R/IRS1 signaling (16), the AMPK-induced mTOR inhibition through TSC2 (17), and the relief from the known mTOR-mediated feedback-loop inhibition mechanism (5, 8).

AICAr potentiates MTX-induced ER stress in ALL cell lines

One of the mechanisms by which MTX has been shown to induce apoptosis is through production of ROS leading to oxidative stress (18). Generation of ROS accumulation in the cytoplasm has been shown to trigger ER stress and the unfolded protein response (UPR; ref. 19), leading to C/EBP homologous protein (CHOP; ref. 20) and GRP78 (21) expression, cleavage of PARP and apoptosis (22). To investigate the molecular mechanisms that lead to apoptotic death in ALL cells treated with AICAr plus MTX, and the roles of AMPK and Akt signaling in these processes, we first determined whether MTX as a single agent led to ER stress/UPR in CCRF-CEM and Nalm6 cells. For this, CCRF-CEM and Nalm6 cells were treated with increasing concentrations of MTX (0–800 nmol/L) for 24 hours, and analyzed by Western blot for expression of CHOP. Our data show a dose-dependent induction of CHOP expression in both ALL cell lines (Fig. 3A). The induction of CHOP at lower doses in Nalm6 cells correlated with their higher sensitivity to MTX compared with CCRF-CEM cells. Next, we analyzed CCRF-CEM and Nalm6 cells treated with AICAr, MTX, and AICAr plus MTX, for accumulation of ROS. Consistent with our data and published results, treatment with MTX for 24 hours induced increased ROS accumulation in both ALL cell lines (Fig. 3B; ref. 18). Of note, exposure of ALL cells to AICAr alone at 200 μmol/L for 24 hours was insufficient to induce any appreciable increase of ROS (Fig. 3B) or CHOP (Fig. 3C), but in contrast, when these same cells were exposed to AICAr at higher concentrations and for longer time (48 hours), a substantial increase in ROS accumulation was also observed (data not shown). As shown in Fig. 2B, treatment with MTX plus AICAr at 200 μmol/L significantly increased ROS generation compared with treatment with MTX alone (ANOVA, $P < 0.01$ for both cell lines), and resulted in significant potentiation of CHOP and GRP78 expression, leading to the concomitant cleavage of PARP in both CCRF-CEM and Nalm6 cells (Fig. 3C). Therefore, the statistically significant increase in apoptosis induced by the combination of AICAr plus MTX in ALL cells (Fig. 2A and B) seems mediated via ROS-induced ER stress and UPR-dependent induction of apoptotic cell death markers.

N-Acetyl-L-cysteine alleviates AICAr plus MTX-induced ER stress and apoptosis in ALL

To test whether ROS accumulation was indeed involved in AICAr and MTX-induced ER stress and apoptosis in ALL cells, we employed NAC, a powerful antioxidant known to scavenge and neutralize ROS (23). For this, CCRF-CEM and Nalm6 cells were treated with AICAr, MTX, or AICAr plus MTX (as described under Materials and Methods) in the presence or absence of NAC (2 mmol/L for CCRF-CEM and 5 mmol/L for Nalm6). Cells were harvested after 24 hours of drug exposure and levels of GRP78 and CHOP expression were determined by Western blotting to assess if commitment to cell death occurred early after drug treatment. Apoptosis was determined by AnnexinV/PI staining after 24, 48, and 72 hours of continuous exposure. Our data show that NAC significantly reduced AICAr and MTX-induced apoptosis in both CCRF-CEM and Nalm6 cells as compared with controls (Fig. 4A and B; ANOVA, $P < 0.01$). In addition, NAC reduced AICAr and MTX-induced ER stress/UPR, as evidenced by decreased CHOP and GRP78 expression in cells cotreated with the antioxidant. The effect of NAC was most pronounced in Nalm6 cells and evidenced as early as 24 hours in comparison with cells treated with MTX or AICAr+MTX in the presence of absence of NAC (Fig. 4B, ANOVA, $P < 0.01$). As it was the case for the cytotoxicity experiments (Fig. 2), CCRF-CEM cells only showed significant reduction in apoptosis after 48 and 72 hours cotreatment with NAC (Fig. 4A, ANOVA, $P < 0.05$ and $P < 0.01$, respectively).

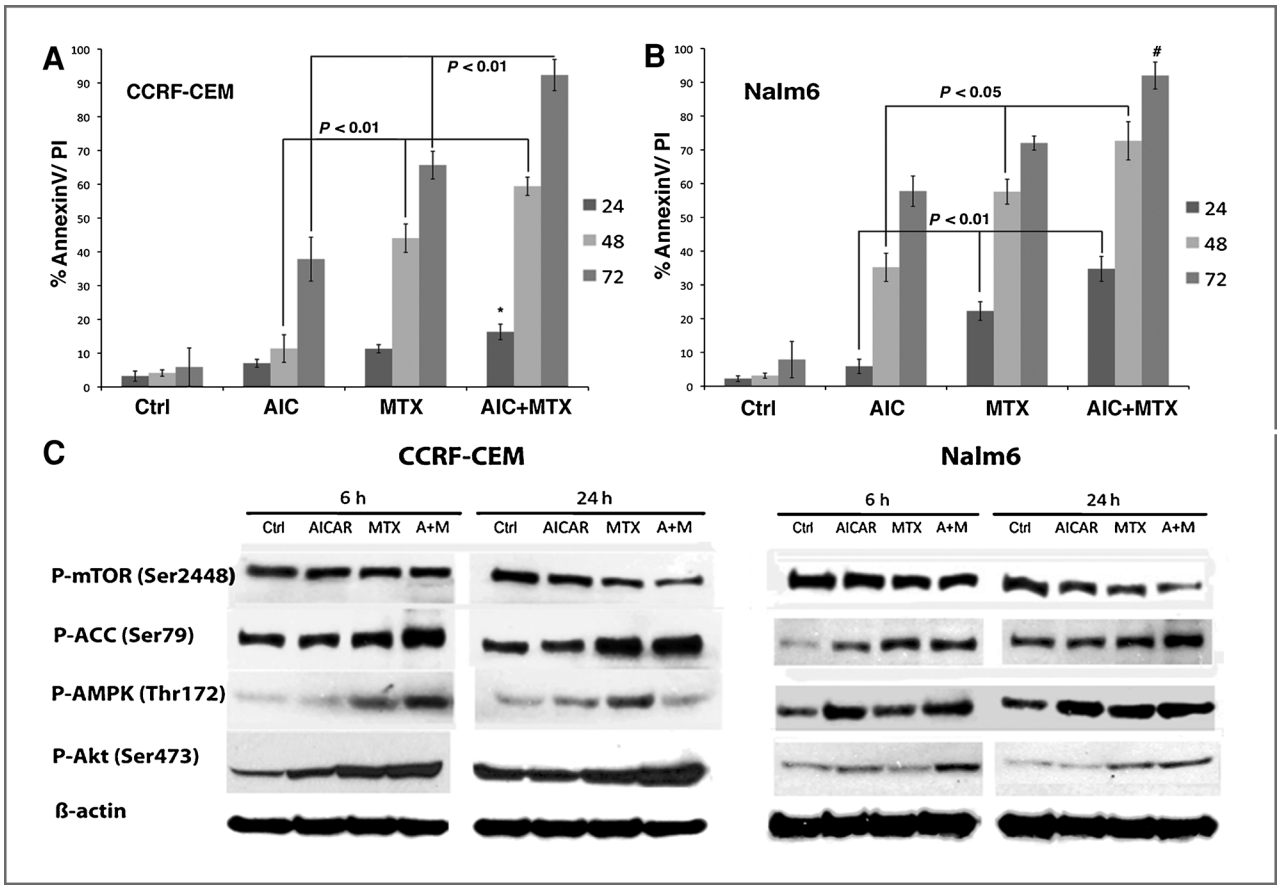

Figure 2. MTX potentiates AICAR-induced cytotoxicity, AMPK and Akt activation, and mTOR downregulation in ALL cell lines. Cells were treated for 24, 48, and 72 hours with AICAr, MTX, and AICAr plus MTX, and apoptosis was assayed at each time point by AnnexinV/PI staining using flow cytometry. AICAr plus MTX lead to significant enhancement of apoptosis in CCRF-CEM ($P < 0.01$ at 48 and 72 hours; (A) and Nalm6 ($P < 0.01$ and 0.02 at 24 and 48 hours, respectively; (B) cells compared with each drug alone. Cells treated as described under Materials and Methods for 6 and 24 hours were analyzed by Western blotting at each time point. MTX potentiates AICAr-induced AMPK activation, mTOR inhibition, and Akt activation in ALL cell lines (C). Graphs represent mean and SE derived from 5 independent experiments. *P* values were calculated by 1-way ANOVA analysis of each drug and the combination at 48 and 72 hours time points.

Salubrinal blocks AICAr plus MTX-induced ER stress and alleviates apoptosis in ALL

To assess the role of ER stress in AICAr plus MTX-induced apoptosis in ALL cell models, we used Salubrinal to pharmacologically block ER stress. Salubrinal has been shown to decrease ER stress-induced apoptosis in response to various ER-stress inducers in multiple cell models by inhibiting dephosphorylation of eIF2α and subsequently blocking global protein synthesis to reduce the strain on the ER lumen (24–26). CCRF-CEM and Nalm6 cells were treated with AICAr, MTX, or AICAr plus MTX in the presence or absence of 10 μmol/L Salubrinal. Apoptosis was determined by AnnexinV/PI staining after 24, 48, and 72 hours of continuous drug exposure. Our data show that Salubrinal significantly reduced AICAr and MTX-induced ER-stress and apoptosis in both CCRF-CEM and Nalm6 cells ($P < 0.01$ at 72 hours for both cell lines; Fig. 5). The rescue effect of Salubrinal was evident in CCRF-CEM only after 48 hours of continuous exposure, whereas in Nalm6 cells the rescue effects were observed as early as 24 hours, and persisted throughout the 72 hours exposure (Fig. 5A and B).

To confirm that the rescue effects of Salubrinal were mediated by alleviation of ER stress/UPR, expression of p-eIF2α, GRP78, and CHOP were assayed by Western blotting. Cotreatment with Salubrinal resulted in decreased expression of the ER stress/UPR markers GRP78 and CHOP, and consistent with the known mechanism of action of this agent, expression of p-eIF2α was increased in Salubrinal treated cells (Fig. 5C). These data showed that AICAr and MTX-induced ER stress/UPR is the mechanism responsible for apoptotic cell death in CCRF-CEM and Nalm6 cells treated with this combination.

Inhibition of Akt and the concomitant potentiation of AMPK alleviate AICAr plus MTX-induced ER stress and cytotoxicity in ALL cells

Akt has been shown to be an effective cellular antagonist of AMPK (27–29). We hypothesized that the

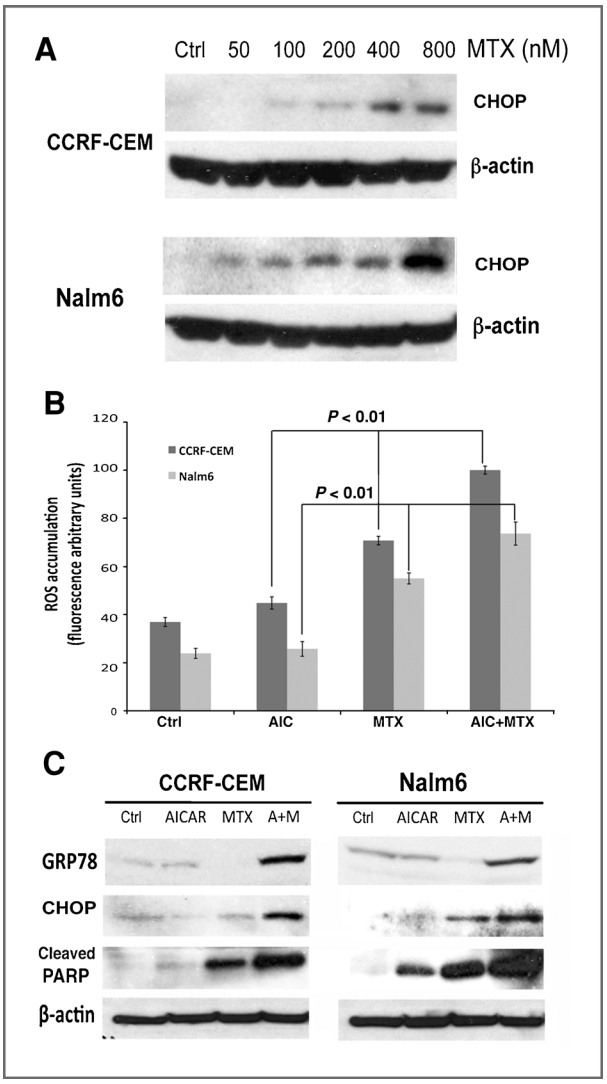

Figure 3. AICAr potentiates MTX-induced ROS accumulation and induction of ER stress in ALL cell lines: Cells were treated with increasing concentrations of MTX for 24 hours, lysed, immunoblotted, and probed with antibody against CHOP (A). Cells were then treated with AICAr, MTX, and AICAr plus MTX combination for 24 hours and assayed for ROS accumulation (B), and the ER stress-specific CHOP, GRP78 and cleaved PARP expression (C), as described in the Materials and Methods. Data in the graphs represent mean and SE from 3 independent experiments. The *P* values shown on the graph were calculated by 1-way ANOVA analysis of each drug and the combination at 24 hours time points. Immunoblots shown are representative of these 3 independent experiments.

observed AICAr plus MTX-induced mTOR inhibition, ER stress/UPR signaling pathways, and increased cell death would be potentiated by inhibition of Akt signaling. To test this hypothesis we determined the role of Akt activation in ALL cells treated with AICAr plus MTX. CCRF-CEM and Nalm6 cells were treated with AICAr, MTX, or AICAr plus MTX (as described under Materials and Methods) in the presence or absence of 12μmol/L AIX for 24 hours and expression of p-AMPK, p-ACC, p-Akt, p-mTOR were determined by Western blotting. As shown in Fig. 6A, cotreatment with AIX (+AIX blots) led to significant abrogation of activated Akt (p-Akt) in both cells lines under all treatment conditions. Akt inhibition after cotreatment with AIX for 24 hours resulted in significant increase in p-AMPK/p-ACC in CCRF-CEM and Nalm6 cells treated with AICAR, MTX, or the combination, and to a more significant downregulation of p-mTOR compared with single drug treatment (Fig. 6A). These signaling changes are consistent with the known effects of Akt on the AMPK signaling factors examined (27–30).

We then determined how Akt inhibition and upregulation of AMPK influenced ER stress and UPR induction in AICAr plus MTX treated cells. For this, we analyzed expression of the ER stress/UPR markers CHOP, GRP78, and the apoptotic marker PARP in ALL cells cotreated with AIX. As shown in Figure 6B, when CCRF-CEM and Nalm6 cells were treated with AICAr, MTX, AICAr plus MTX in the presence of AIX, expression of CHOP, GRP78, and cleavage of PARP were significantly decreased, suggesting that upregulation of AMPK and downregulation of Akt may attenuate ER stress/UPR in ALL cells. This decrease in ER stress/UPR markers correlated with a 50% abrogation of cell death in both cell lines (Fig. 6C and D). Consequently, our data suggest that Akt inhibition concomitant to AICAr plus MTX-induced upregulation of AMPK relieves ER stress/UPR-induced apoptosis in these ALL models, indicating that the contextual cross-talk between AMPK and Akt are important in determining ALL cell fate through ER stress/UPR related mechanisms.

shRNA knockdown of AMPK promotes ER stress and sensitizes ALL cells to AICAr plus MTX-induced cytotoxicity

In order to gain additional insight into the paradoxical proapoptotic and prosurvival functions ascribed to AMPK and its role in the relief of ER stress/UPR and cytotoxicity under our experimental conditions, we employed lentivirus encoding shRNA against the α1 and α2 subunits of AMPK to knockdown total AMPK protein levels in both ALL cell lines. Lentiviral-transduced ALL cells were then treated with AICAr, MTX, and AICAr plus MTX in combination for 24 hours (as described under Materials and Methods), lysed, immunoblotted, and probed with antibodies against p-AMPK (Thr172), GRP78, CHOP, and PARP. We found that lentiviral shRNA-mediated knockdown of AMPK significantly sensitized both ALL cell lines to AICAr plus MTX-induced ER stress/UPR, as assessed by increased CHOP and GRP78 expression (Fig. 7A and B). Consequently, AMPK knockdown potentiated the AICAr, MTX, and AICAr plus MTX induction of apoptosis, as assessed by increased PARP cleavage (Fig. 7A and B) and increased cell death (Fig. 7C and D). Therefore, in these ALL cell line models AMPK signaling also seems necessary in the regulation of ER stress/UPR.

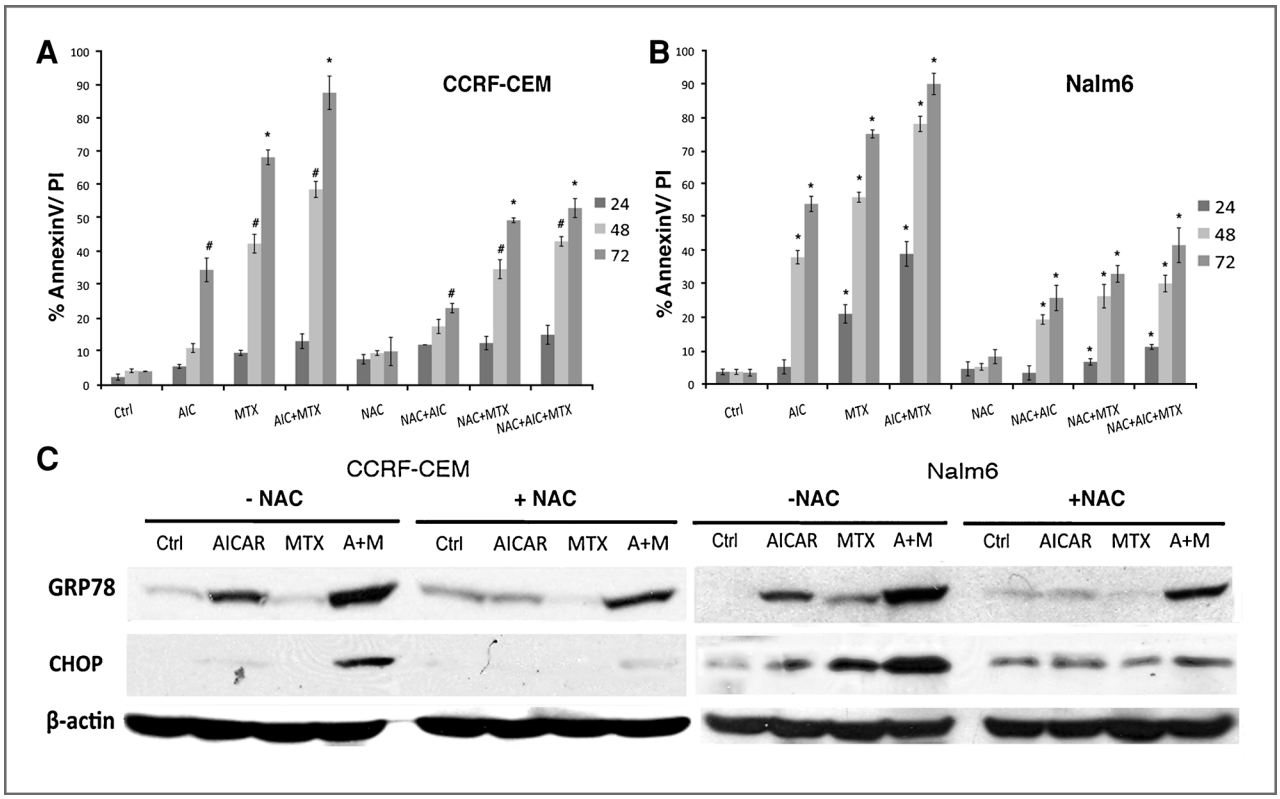

Figure 4. N-Acetyl-L-cysteine alleviates AICAr plus MTX-induced ER stress and apoptosis in ALL. Cells were treated with AICAr, MTX, or AICAr plus MTX (as described under Materials and Methods) in the presence or absence of 2 mmol/L or 5 mmol/L NAC for CCRF-CEM (A) and Nalm6 (B), respectively. Cells were harvested after 24 hours of drug exposure and levels of GRP78 and CHOP were determined by Western blotting (C). Apoptosis was determined by AnnexinV staining after 24, 48, and 72 hours of continuous exposure. Data in the graphs represent mean and SE of 3 independent experiments. *P* values: * corresponds to $P < 0.01$ and # to $P < 0.05$. *P* values were calculated by 1-way ANOVA analysis of each drug/combination in the presence versus absence of NAC at each time point.

These data and that presented in Fig. 6 suggest that under these experimental conditions, concomitant activation AMPK protects ALL cells from ER stress-induced cytotoxicity.

Discussion

The antiproliferative properties of AMPK have become evident with the discovery of the upstream kinase LKB1 and the downstream factor TSC2. Mutations in either LKB1 or TSC2 result in similar clinical syndromes: increased incidence of gastrointestinal polyps, benign tumors, and higher chances of malignant tumor formation, although phenotypes are restricted to different organs (31, 32). Although AMPK modulated activity can be tissue specific, in general, AMPK activation results in inhibition of lipid, glycogen, and protein synthesis as well as cell growth inhibition and proliferation, whereas fatty acid oxidation and glucose uptake are concomitantly stimulated [reviewed in (7)]. In certain cells and under certain conditions, these AMPK-perturbed processes result in protective and prosurvival effects. For instance, AICAr has been shown to protect cardiac cells from injury and apoptosis caused by myocardial ischemia in humans (33). In most cited cases, AMPK exerts protective effects in cells with a resting phenotype where a decrease in metabolic rate does not alter the balance between survival and death; however, in fast-growing and cancer cells that exhibit elevated anabolic rates, inhibition of ATP-catabolic processes by AMPK is incompatible with survival and often leads to apoptosis (reviewed in (17). Nevertheless, AMPK activation has been shown to promote metabolic changes to maintain cell proliferation and survival in human prostate cancer cells (34), and to protect epithelial cells from TRAIL-induced apoptosis (35). Therefore, paradoxical prosurvival and proapoptotic functions have been described for AMPK, which tend to be tissue specific, and highlight the regulatory complexities of this kinase and related signaling pathways.

Our laboratory has previously described the cytotoxic effects of AICAr on Bp- and T-ALL cell lines, and shown that AICAr inhibited cell proliferation, induced cell cycle arrest, and apoptosis in multiple ALL cell lines. Using the adenosine inhibitor iodotubericidin, which blocks conversion of exogenous AICAr to AICAR (ZMP), we confirmed AICAr's conversion to the AMP-mimetic ZMP is essential for AICAr-induced cytotoxicity in ALL (8).

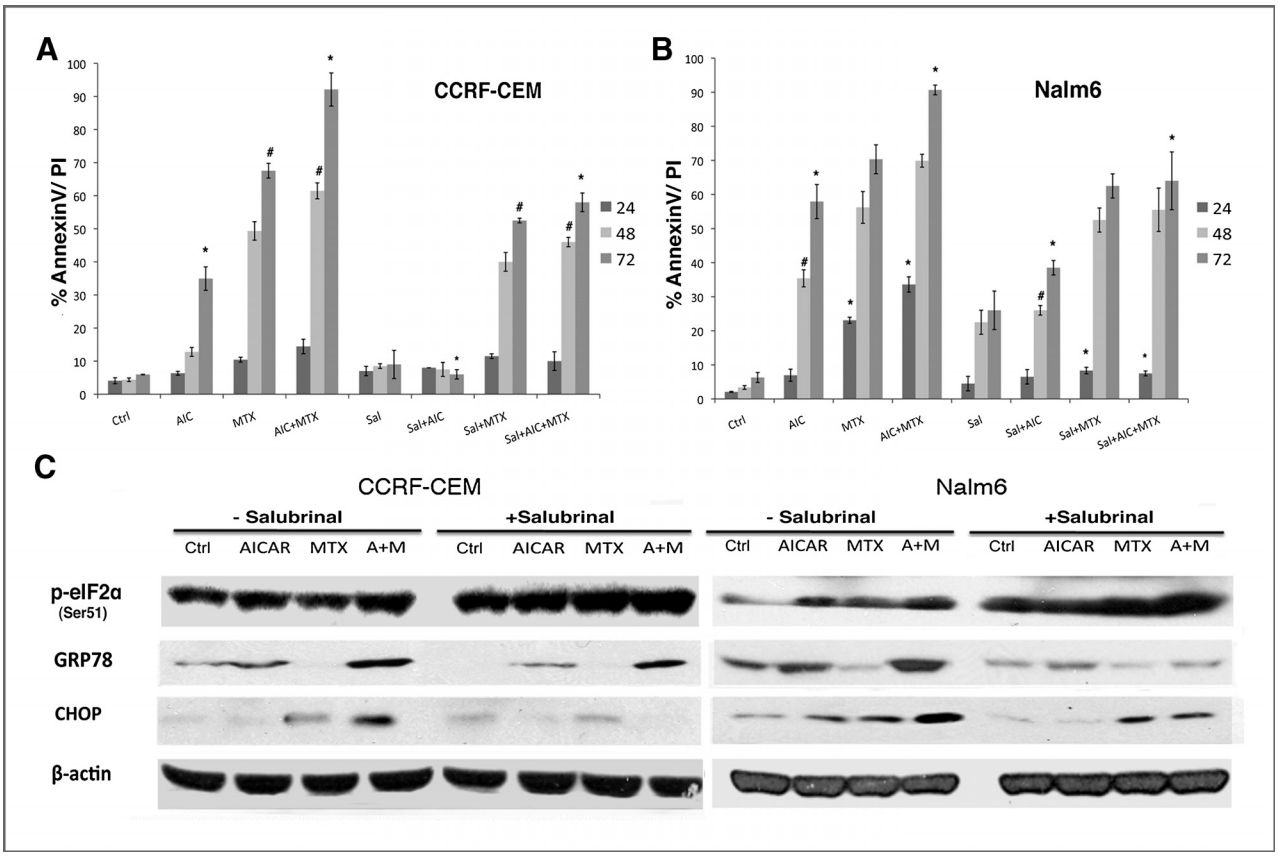

Figure 5. ER-stress inhibition alleviates AICAr plus MTX-induced ER stress and apoptosis in ALL. CCRF-CEM (A) and Nalm6 (B) ALL cells were treated with AICAr, MTX, or AICAr plus MTX (as described under Materials and Methods) in the presence or absence of 10 μmol/L Salubrinal, harvested after 24 hours of drug exposure, and levels of GRP78, CHOP, and eIF2α were determined by Western blotting (C). Apoptosis was determined by AnnexinV staining after 24, 48, and 72 hours of continuous exposure. Data in the graphs represent mean and SE of 3 independent experiments. *P* values: * corresponds to $P < 0.01$ and # to $P < 0.05$. *P* values were calculated by 1-way ANOVA analysis of each drug/combination in the presence versus absence of Salubrinal at a given time point.

Beckers et al. have shown that MTX markedly sensitizes AMPK for activation by AICAr, and enhances AICAr-induced inhibition of tumor-associated anabolism and colony formation in breast cancer, epidermoid carcinoma, and prostate cancer cell lines (11). Herein we have shown that similarly, MTX treatment resulted in enhanced AICAr-induced AMPK activation in T- and Bp-ALL cell lines, and that these effects translated to downstream targets such as activation of ACC (p-ACC) and inhibition of mTOR (Fig. 2C). For each of these signaling factors, the combination of AICAr plus MTX resulted in increased perturbations of their phosphorylation status and correlated with a greater induction of cell death compared with each drug alone. Nevertheless, Although Bp-ALL cells exhibited increased apoptosis after combination therapy as early as 24 hours (Fig. 2B), T-ALL cells required at least 48 hours for increased apoptosis (Fig. 2A). These differences may result from differences in signaling within AMPK and related PI3K/Akt pathways in the PTEN mutant CCRF-CEM cells and/or could be secondary to known differences in the metabolism of drugs such as MTX in Bp- and T-ALL.

Our data also highlight the importance of the cross-talk between AMPK and oncogenic networks such as PI3K/Akt and mTOR. We previously observed that cells treated with increasing concentrations of AICAr exhibited higher levels of Akt phosphorylation as compared with untreated/control cells, and this effect was dose dependent (8). In this report we uncovered for the first time, that AICAr in combination with MTX significantly induces Akt phosphorylation at residue Ser473 in both CCRF-CEM and Nalm6 cells (Fig. 2C), and phosphorylation at Thr308 in CCRF-CEM cell line only (data not shown). We postulate that the differences in p-Akt expression in these cell lines reflects differences in PTEN expression and resulting downstream Akt activations, as CCRF-CEM cells express an inactivating mutation in PTEN leading to higher constitutive activation of Akt signaling, whereas Nalm6 cells express wild-type PTEN. Furthermore, we have shown that inhibition of Akt with the pharmacological inhibitor of Akt leads to a significant increase in AMPK activation in both ALL cell lines (Fig. 6A). We recently reported that the cross-talk between AMPK and Akt is bidirectional, and that AMPK-induced activation of Akt by AICAr is mediated

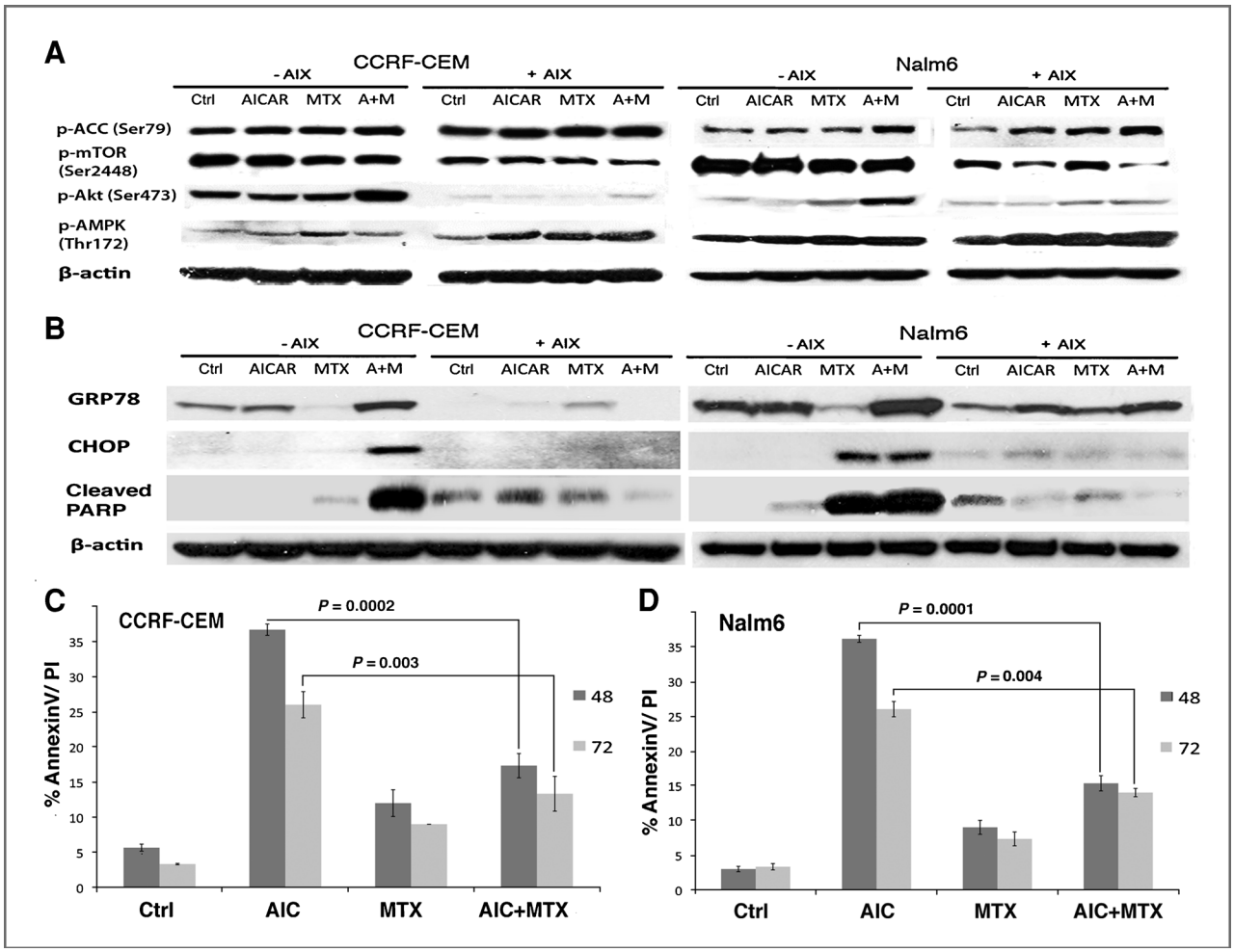

Figure 6. Inhibition of Akt and the concomitant potentiation of AMPK alleviate AICAr plus MTX-induced ER stress and cytotoxicity in ALL cell lines: CCRF-CEM and Nalm6 cells were treated as described under Materials and Methods in the presence 12 μmol/L Akt inhibitor X (+AIX) and absence (-AIX). Equal aliquots of protein extracts were analyzed by Western blotting for AMPK (Thr172), ACC (Ser79), mTOR (Ser2448), Akt (Ser472), CHOP, GRP78, and cleaved PARP (A, B). CCRF-CEM and Nalm6 cell death was assessed by AnnexinV staining and flow cytometry at 48 and 72 hours (C, D). The data represent mean and SE from 3 independent experiments. The *P* values shown on the graphs were calculated with 2-tailed paired *t* Test analysis of AICAR plus MTX combination in the presence versus absence of AIX at each time point.

by IGF-1R dependent and independent mechanisms in ALL (36).

In this report, we have shown that MTX induces a dose-dependent induction of CHOP expression in ALL cells, an ER-stress/UPR marker indicative of commitment to apoptosis (Fig. 3A). These data are consistent with the recently reported induction of UPR in the promyelocytic leukemia cell line HL60 following NFkB targeting with MTX (37). More important, employing the antioxidant NAC and ER-stress inhibitor Salubrinal, we have shown for the first time that the significant increase in induction of apoptotic death attributed to the combination of AICAr plus MTX in ALL cells results from enhanced accumulation of ROS/oxidative stress leading to induction of UPR/ER stress (Figs. 3, Fig. 4, Fig. 5).

Altogether our findings describe the ability of AICAr and MTX to perturb 3 major cellular pathways: AMPK, Akt, and UPR/ER stress pathways. MTX potentiates the ability of the AMP-analogue AICAR to activate AMPK by increasing the total levels of AMP and by decreasing the total levels of ATP (10, 11, 38). At the same time, AICAr potentiates MTX-induced ER stress via upregulation of ROS accumulation. Consequently, we postulate that AICAr plus MTX-induced ER stress in conjunction with the upregulation of Akt, which negatively regulates AMPK, leads to prolonged ER stress and subsequent cell death. In this context, activated Akt exerts a proapoptotic effect in our experimental model, that is when Akt is inhibited and AMPK activity is increased, AICAr plus MTX-induced ER stress is alleviated decreasing cell death (Fig. 6). Therefore, we suggest that the described paradoxical prosurvival and proapoptotic responses following AMPK and Akt activation result from the intracellular signaling context within these pathways in cells at the

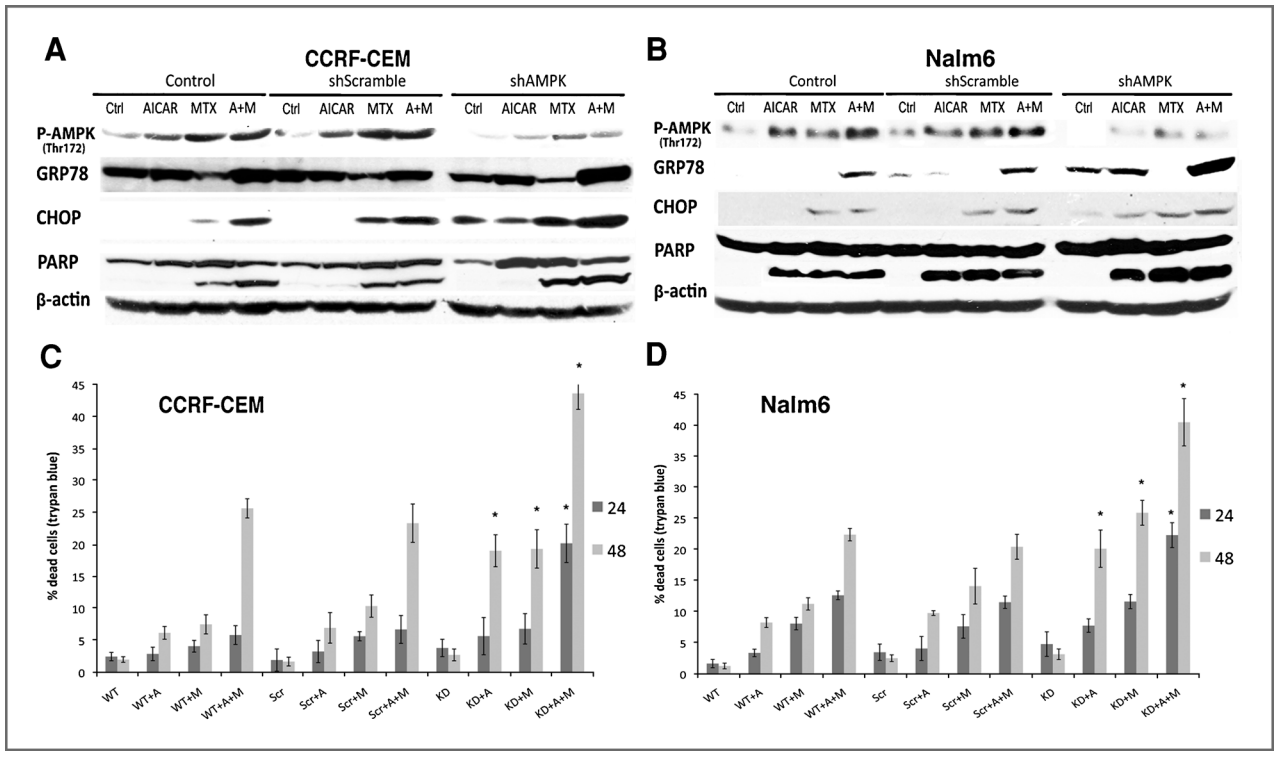

Figure 7. shRNA knockdown of AMPK promotes AICAr plus MTX-induced ER stress and apoptosis in both ALL cell lines: CCRF-CEM (A) and Nalm6 (B) cells were transduced with lentivirus encoding shScramble (Scr) or shAMPK (Knockdown, KD), and treated as described under Materials and Methods. Mock-transduced cells were used as control. Cells were lysed, immunoblotted, and probed with antibodies specific to p-AMPK (Thr172), GRP78, CHOP, and PARP (A, B). Cytotoxicity data were obtained by an automated trypan blue exclusion assay as described in the Materials and Methods (C, D). Data in the graphs represent mean and SE of 3 independent experiments. *P* values were calculated by 1-way ANOVA followed by the Newman-Keuls multiple comparison test for each drug or combination in shScramble- vs. shAMPK-expressing cells at a given time point. * corresponds to $P < 0.01$.

time of drug-induced injury. In conclusion, our data underscore the complexity of the interactions within these pathways, and suggest that the contextual relationship between these signaling proteins and cross-talk with related pathways are critical determinants of cellular responses and fate (survival vs. death) in ALL cells. Consequently, our findings provide a strong rationale for cotargeting strategies that achieve maximal induction of apoptotic death, as an important strategy for clinical translation in future ALL trials.

Disclosure of Potential Conflicts of Interest

No potential conflicts of interest were disclosed.

Acknowledgments

The authors would like to thank Dr. Bart Kamen for insightful discussions, and Joanna DeSalvo and Dr. Jianfeng Du for helpful input.

Grant Support

This investigation was supported by the National Cancer Institute (NCI R01-CA098152) and the Leukemia & Lymphoma Society Translational Research Program Grant (6168–09).

The costs of publication of this article were defrayed in part by the payment of page charges. This article must therefore be hereby marked *advertisement* in accordance with 18 U.S.C. Section 1734 solely to indicate this fact.

Received August 20, 2010; revised December 28, 2010; accepted January 4, 2011; published OnlineFirst January 24, 2011.

References

1. Pui CH, Evans WE. Acute lymphoblastic leukemia N. Engl J Med 1998;339:605–15.
2. Greaves M. Childhood leukaemia. Bmj 2002;324:283–7.
3. Pui CH, Evans WE. Treatment of acute lymphoblastic leukemia. N Engl J Med 2006;354:166–78.
4. Hardie DG, Carling D. The AMP-activated protein kinase–fuel gauge of the mammalian cell? Eur J Biochem 1997;246:259–73.
5. Kemp BE, Mitchelhill KI, Stapleton D, Michell BJ, Chen ZP, Witters LA. Dealing with energy demand: the AMP-activated protein kinase. Trends Biochem Sci 1999;24:22–5.
6. Hawley SA, Boudeau J, Reid JL, Mustard KJ, Udd L, Mäkelä TP, et al. Complexes between the LKB1 tumor suppressor, STRAD alpha/beta and MO25 alpha/beta are upstream kinases in the AMP-activated protein kinase cascade. J Biol 2003;2:28–44.

7. Guigas B, Bertrand L, Taleux N, Foretz M, Wiernsperger N, Vertommen D, et al. 5-aminoimidazole-4-carboxamide-1-beta-D-ribofuranoside and metformin inhibit hepatic glucose phosphorylation by an AMP-activated protein kinase-independent effect on glucokinase translocation. Diabetes 2006;55:865–74.
8. Sengupta TK, Leclerc GM, Hsieh Kinser TT, Leclerc GJ, Singh I, Barredo JC. Cytotoxic effect of 5-aminoimidazole-4-carboxamide-1-beta-4-ribofuranoside (AICAR) on childhood acute lymphoblastic leukemia (ALL) cells: implication for targeted therapy. Mol Cancer 2007;6:46–58.
9. Cronstein BN, Naime D, Ostad E. The antiinflammatory mechanism of methotrexate. increased adenosine release at inflamed sites diminishes leukocyte accumulation in an in vivo model of inflammation. J Clin Invest 1993;92:2675–82.
10. Adams J, Chen ZP, Van Denderen BJ, Morton CJ, Parker MW, Witters LA, et al. Intrasteric control of AMPK via the γ1 subunit AMP allosteric regulatory site. Protein Sci 2004;13:155–65.
11. Beckers A, Organe S, Timmermans L, Vanderhoydonc F, Deboel L, Derua R, et al. Methotrexate enhances the antianabolic and antiproliferative effects of 5-aminoimidazole-4-carboxamide riboside. Mol Cancer Ther 2006;5:2211–7.
12. Racanelli AC, Rothbart SB, Heyer CL, Moran RG. Therapeutics by cytotoxic metabolite accumulation: pemetrexed causes ZMP accumulation, AMPK activation, and mammalian target of rapamycin inhibition. Cancer Res 2009;69:5467–74.
13. Barredo JC, Synold TW, Laver J, Relling MV, Pui CH, Priest DG, et al. Differences in constitutive and post-methotrexate folylpolyglutamate synthetase activity in B-lineage and T-lineage leukemia. Blood 1994;84:564–9.
14. Galpin AJ, Schuetz JD, Masson E, Yanishevski Y, Synold TW, Barredo JC, et al. Differences in folylpolyglutamate synthetase and dihydrofolate reductase expression in human B-lineage versus T-lineage leukemic lymphoblasts: Mechanisms for lineage differences in methotrexate polyglutamylation and cytotoxicity. Mol Pharmacol 1997; 52:155–63.
15. Palomero Teresa, Sulis M Luisa, Cortina Maria, Real PJ, Barnes K, Ciofani M, et al. Mutational loss of PTEN induces resistance to NOTCH1 inhibition in T-cell leukemia.Nat Med 2007;13:1203–10.
16. Jakobsen SN, Hardie DG, Morrice N, Tornqvist HE. 5′-AMP-activated protein kinase phosphorylates IRS-1 on ser-789 in mouse C2C12 myotubes in response to 5-aminoimidazole-4-carboxamide riboside. J Biol Chem 2001;276:46912–6.
17. Motoshima H, Goldstein BJ, Igata M, Araki E. AMPK and cell proliferation–AMPK as a therapeutic target for atherosclerosis and cancer. J Physiol 2006;574:63–71.
18. Herman S, Zurgil N, Deutsch M. Low dose methotrexate induces apoptosis with reactive oxygen species involvement in T lymphocytic cell lines to a greater extent than in monocytic lines. Inflamm Res 2005;54:273–80.
19. Guan L, Han B, Li Z, Hua F, Huang F, Wei W, et al. Sodium selenite induces apoptosis by ROS-mediated endoplasmic reticulum stress and mitochondrial dysfunction in human acute promyelocytic leukemia NB4 cells. Apoptosis 2009;14:218–25.
20. Terai K, Hiramoto Y, Masaki M, Sugiyama S, Kuroda T, Hori M, et al. AMP-activated protein kinase protects cardiomyocytes against hypoxic injury through attenuation of endoplasmic reticulum stress. Mol Cell Biol 2005;25:9554–75.
21. Lai MT, Huang KL, Chang WM, Lai YK. Geldanamycin induction of grp78 requires activation of reactive oxygen species via ER stress responsive elements in 9L rat brain tumour cells. Cell Signal 2003;15:585–95.
22. Oliver FJ, de la Rubia G, Rolli V, Ruiz-Ruiz MC, de Murcia G, Murcia JM. Importance of poly(ADP-ribose) polymerase and its cleavage in apoptosis. lesson from an uncleavable mutant. J Biol Chem 1998;273:33533–9.
23. Spagnuolo G, D'Antò V, Cosentino C, Schmalz G, Schweikl H, Rengo S. Effect of N-Acetyl-l-cysteine on ROS production and cell death caused by HEMA in human primary gingival fibroblasts. Biomaterials 2006;27:1803–9.
24. Eom KS, Kim HJ, So HS, Park R, Kim TY. Berberine-induced apoptosis in human glioblastoma T98G cells is mediated by endoplasmic reticulum stress accompanying reactive oxygen species and mitochondrial dysfunction. Biol Pharm Bull 2010;33:1644–9.
25. Wang Q, Jiang H, Fan Y, et al. Phosphorylation of the α-subunit of the eukaryotic initiation factor-2 (eIF2α) alleviates benzo[a]pyrene-7,8-diol-9,10-epoxide induced cell cycle arrest and apoptosis in human cells. Environ Toxicol Pharmacol. In press.
26. Zbidi H, Redondo PC, López JJ, Bartegi A, Salido GM, Rosado JA. Homocysteine induces caspase activation by endoplasmic reticulum stress in platelets from type 2 diabetics and healthy donors. Thromb Haemost 2010;103:1022–32.
27. Horman S, Vertommen D, Heath R, Neumann D, Mouton V, Woods A, et al. Insulin antagonizes ischemia-induced Thr172 phosphorylation of AMP-activated protein kinase alpha-subunits in heart via hierarchical phosphorylation of Ser485/491. J Biol Chem 2006 Mar 3;281:5335–40.
28. Berggreen C, Gormand A, Omar B, Degerman E, Goransson O. Protein kinase B activity is required for the effects of insulin on lipid metabolism in adipocytes. Am J Physiol Endocrinol Metab 2009;296: E635–46.
29. Hahn-Windgassen A, Nogueira V, Chen CC, Skeen JE, Sonenberg N, Hay N. Akt activates the mammalian target of rapamycin by regulating cellular ATP level and AMPK activity. J Biol Chem 2005;280:32081–9.
30. Shi Y, Yan H, Frost P, Gera J, Lichtenstein A. Mammalian target of rapamycin inhibitors activate AKT kinase in multiple myeloma cells by up-regulating the insulin-like growth factor receptor/insulin receptor substrate-1/phosphatidylinositol 3-kinase cascade. Mol Cancer Ther 2005;4:1533–40.
31. Hemminki A, Markie D, Tomlinson I, Avizienyte E, Roth S, Loukola A, et al. A serine/threonine kinase gene defective in peutz-jeghers syndrome. Nature 1998;391:184–7.
32. Nakanishi C, Yamaguchi T, Iijima T, Saji S, Toi M, Mori T, et al. Germline mutation of the LKB1/STK11 gene with loss of the normal allele in an aggressive breast cancer of peutz-jeghers syndrome. Oncology 2004;67:476–9.
33. Mullane K. Acadesine: the prototype adenosine regulating agent for reducing myocardial ischaemic injury. Cardiovasc Res 1993;27:43–7.
34. Park HU, Suy S, Danner M, Dailey V, Zhang Y, Li H, et al. AMP-activated protein kinase promotes human prostate cancer cell growth and survival. Mol Cancer Ther 2009;8:733–41.
35. Herrero-Martin Griselda, Hoyer-Hansen Maria, Garcia-Garcia Celina, Fumarola C, Farkas T, López-Rivas A, et al. TAK1 activates AMPK-dependent cytoprotective autophagy in TRAIL-treated epithelial cells. EMBO J 2009;28:677–85.
36. Leclerc GM, Leclerc GJ, Fu G, Barredo JC. AMPK-induced activation of Akt by AICAR is mediated by IGF-1R dependent and independent mechanisms in acute lymphoblastic leukemia. J Mol Signal 2010;5:15–28.
37. Agarwal NK, Mueller GA, Mueller C, Streich JH, Asif AR, Dihazi H. Expression proteomics of acute promyelocytic leukaemia cells treated with methotrexate. Biochim Biophys Acta 2010;1804:918–28.
38. Swinnen JV, Beckers A, Brusselmans K, Organe S, Segers J, Timmermans L, et al. Mimicry of a cellular low energy status blocks tumor cell anabolism and suppresses the malignant phenotype. Cancer Res 2005;65:2441–8.